

Increased Superconducting Transition Temperature of a Niobium Thin Film Proximity Coupled to Gold Nanoparticles Using Linking Organic Molecules

Eran Katzir,¹ Shira Yochelis,¹ Felix Zeides,² Nadav Katz,² Yaov Kalcheim,² Oded Millo,² Gregory Leituss,³ Yuri Myasodeyov,⁴ Boris Ya. Shapiro,⁵ Ron Naaman,⁶ and Yossi Paltiel^{1,*}

¹*Applied Physics Department and the Center for Nano-Science and Nano-Technology, the Hebrew University of Jerusalem, Jerusalem, 91904 Israel*

²*Racah Institute of Physics, the Hebrew University of Jerusalem, Jerusalem, 91904 Israel*

³*Chemical Support, The Weizmann Institute, Rehovot 76100, Israel*

⁴*Department of Physics, The Weizmann Institute of Science, Rehovot, 76100 Israel*

⁵*Physics Department, Bar-Ilan University, Ramat-Gan, 52900 Israel*

⁶*Department of Chemical Physics, The Weizmann Institute of Science, Rehovot, 76100 Israel*

(Received 22 June 2011; revised manuscript received 29 November 2011; published 8 March 2012)

The superconducting critical temperature, T_C , of thin Nb films is significantly modified when gold nanoparticles (NPs) are chemically linked to the Nb film, with a consistent enhancement when using 3 nm long disilane linker molecules. The T_C increases by up to 10% for certain linker length and NP size. No change is observed when the nanoparticles are physisorbed with nonlinking molecules. Electron tunneling spectra acquired on the linked NPs below T_C typically exhibit zero-bias peaks. We attribute these results to a pairing mechanism coupling electrons in the Nb and the NPs, mediated by the organic linkers.

DOI: 10.1103/PhysRevLett.108.107004

PACS numbers: 74.62.Bf, 74.25.Bt, 74.70.Kn, 74.78.-w

The proximity effect (PE) in superconductivity occurs when a superconductor (S) is placed in contact with a normal metal (N). The resulting critical temperature of the superconductor, T_C , is then suppressed and signs of weak superconductivity are induced in N [1]. The PE is well understood for “conventional” BCS superconductors, and is known to take place via Andreev reflections. By this, superconductivity is weakened in the superconductor and superconducting correlations are induced in the normal side up to a distance where the electron and hole lose phase coherence [1]. Hence, the PE requires good electrical contact and Fermi wave vector matching. Nevertheless, and quite surprisingly, PEs were observed also for nonmetallic systems such as Anderson insulators [2], molecules [3], and hybrid superconductor quantum-dot devices [4].

Even more intriguing, and less common, is the inverse PE, where the T_C of a superconductor is increased upon attachment to a nonsuperconducting material. Such an effect was reported for quench-condensed ultrathin Pb film (S), where T_C was increased upon coverage with Ag (N) [5]. The authors attributed their findings to Coulomb repulsion screening. T_C enhancement was recently observed also for S - N underdoped-overdoped bilayers involving cuprate high-temperature superconductors [6].

Here we report the observation of a robust inverse PE effect for a self-assembled monolayer of gold nanoparticles (NPs), attached via organic linker molecules to Nb film [7]. The critical temperature of the Nb film increased substantially in such heterostructures, by up to $\sim 10\%$, compared to the bare film. The relative enhancement is more pronounced when the Nb films are thinner. Concomitantly, tunneling spectra acquired on the linked

Au NPs, below T_C , typically exhibit zero-bias peaks. Only in the case of the shortest linkers, on some Au NPs, superconducting gaps were measured, signifying proximity effect and strong coupling. It is important to note that in contrast to previous bulk planer geometries, the T_C enhancement measured here involves a local effect by the use of metallic nanodots with organic molecules.

In conventional superconductivity, T_C is governed by the interactions leading to electron Cooper pairing. This is in contrast to granular or underdoped high- T_C superconductors, where T_C is governed by phase fluctuations [8]. It is well known that the critical temperature and the gap can be enhanced by a few percent by driving the superconductor out of equilibrium [9]. When the superconductors are carefully arranged, the critical temperature depends not only on the strength of the pairing interactions but also on quasiparticle excitations. Optimizing the tunnel injector-extractor arrangement and the thickness of Al film sandwiched between two tunnel junctions in the Nb-AlO_x-Al-AlO_x-Nb configuration has led to almost 100% enhancement of T_C in the Al (S) layer [10].

In the present work we investigated modifications in the superconductor properties of 150- and 50-nm-thick Nb films due to adsorption of organic molecules and Au NPs. We used two types of Nb films, one evaporated on sapphire and the other sputtered on Si wafers. The T_C of the sputtered film was higher for the same film thickness; nevertheless, both samples gave the same order of T_C enhancement upon the attachment of the Au NPs. The corrugations of the Nb films were of the order of 2–3 nm over an area of few μm^2 . The films were coated with self-assembled monolayers of two types of organic linkers, to

which the Au NPs were attached [see Fig. 1(a)], 3-methylpropane bis-trichlorosilane (disilane), which forms a 3-nm-thick layer, and mercapto propyl silane (MPS), which forms a 0.5-nm-thick monolayer. We also studied a sample covered by ~ 3 nm long nonlinking octadecyl trichlorosilane (OTS) molecules, on which the Au NPs were only physisorbed and thus acted merely as a

spacer layer. All samples were cleaned with Ar plasma followed by an acetone-boiling cleaning procedure prior to the organic layer adsorption. The thicknesses of the organic films were measured using an ellipsometer as well as by x-ray photoelectron spectroscopy (see Supplemental Material [11]). The Au NPs, either 10 or 5 nm in diameter, were attached to the organic molecules using the procedure described in Ref. [12].

The measured T_C values of the 150 nm Nb films ranged from 7.8 to 8.5 K and the magnetic field, normal to the sample surface, could be varied up to 1 T. For the sputtered films, the superconducting transition width was ~ 0.05 K, implying that the Nb films were quite pure. The transition was 2 times wider for the evaporated film. The scanning tunneling microscopy (STM) and spectroscopy measurements were performed in a homebuilt cryogenic STM, using Pt-Ir tips, operating in a clean He exchange-gas environment.

Figure 1(b) presents the derivative of the resistance as a function of temperature, normalized to the T_C of the bare evaporated Nb film of thickness 150 nm, which was 7.8 K. Data for the bare film (black curve) are shown as well as data obtained after the attachment of 5 and 10 nm-diameter Au NPs with different organic linkers. The inset of Fig. 1(b) shows a SEM image of the monolayer made from the 10-nm Au NPs on top of the Nb film. All samples were cooled at zero magnetic fields, and the measurements were performed in the cooling direction using different currents. The results presented are the ones with the highest current for which no heating effect was observed.

When using the Nb film and short (MPS) organic linker, the binding of the Au NPs yields a reduction of the critical temperature. This reduction is more pronounced with the larger NPs (10 nm diameter) as compared with the small ones (5 nm diameter). These results are consistent with the expected PE and occurred also when the Au NPs were physisorbed directly on the surface of the Nb film. However, when longer linker molecules were used, a surprising increase in T_C was observed, 3% for the 10-nm Au NPs and 2% for the 5-nm Au NPs. Similar results were measured using the sputtered Nb film.

Figure 1(c) presents the measurements on the 50-nm-thick sputtered Nb films coated with MPS and disilane molecules to which 10 nm Au NPs were covalent bonded. Here, an increase of about 10% in the critical temperature is measured for the MPS molecule (green curve), comparable to that measured for the disilane molecule (red curve). For comparison, results are shown for the NPs physisorbed on the nonlinking OTS layer (blue curve). A negligible effect on T_C is observed in this case, although the thickness of this layer is comparable to that of disilane. The widening of the critical temperature phase transition fits previous published results [13], where only organic molecules are adsorbed. This observation confirms that screening effects are not involved [5], since here the OTS

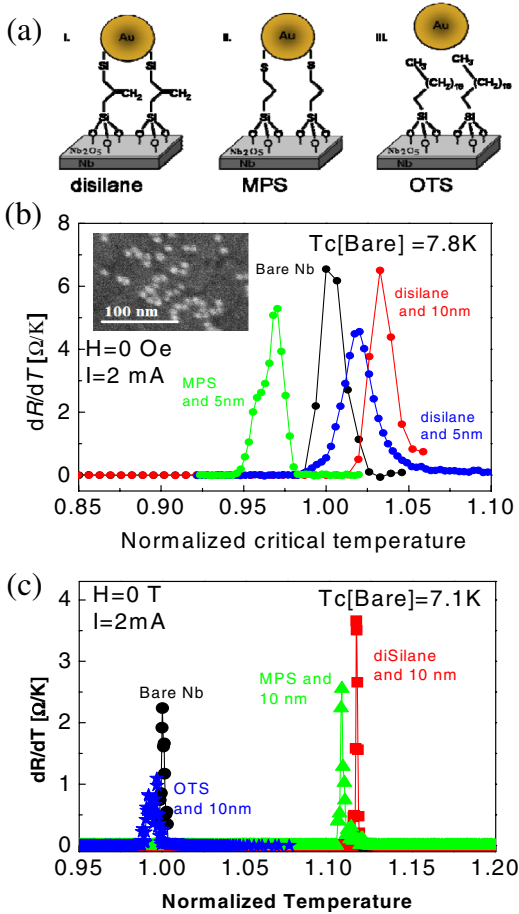


FIG. 1 (color online). (a) Schematics of the samples: Self-assembled monolayers of three types of molecules adsorbed on top of Nb films. (I) 3-methylpropane bis-trichlorosilane (disilane), which forms a 3-nm-thick layer, (II) mercapto propyl silane (MPS), forming a 0.5-nm-thick monolayer, and (III) trichloro(octadecyl)silane (OTS) forming a 3-nm-thick layer. The Au nanoparticles were chemically linked only to the first two types of molecules. (b) The differential resistance as a function of the normalized temperature. The temperature is normalized to T_C of the corresponding bare evaporated 150-nm-thick Nb film (black curve). The blue and red curves show results obtained for samples with 5 and 10 nm Au NPs, respectively, linked to the Nb film via disilane molecules. In green, data for 5 nm NPs linked by the MPS organic monolayer. The inset shows a SEM image of the Au NPs adsorbed on top of the Nb film. (c) 50 nm sputtered Nb film coated with 10 nm NPs linked by the disilane and MPS organic layer showing about 10% increase in T_C . Very small changes in the critical temperature are observed when using nonlinking OTS molecules.

layer acts only as a spacer. We also find that the adsorbed monolayer by itself, with no NPs, does not affect the critical temperature consistent with Ref. [13]. The increase in the critical temperature was similar for both the sputtered film with higher T_C and the evaporated film of the same thickness. Since the adsorption of NPs is not uniform, it leads to local fluctuations of the critical current [14] and probably to local T_C fluctuations. This effect could be used for patterning areas with high T_C on the Nb film, by selective adsorption of the NPs.

The dependence of T_C on the density of the adsorbed Au NPs is demonstrated in Fig. 2, where the temperature dependent resistance, $R(T)$, is presented for different NP densities. After deposition of 10-nm-diameter Au NPs on the disilane layer, T_C increased by 3% as compared with the bare Nb substrate. Removing the covalent bonded NPs is difficult, and only by applying plasma cleaning we were able to affect the organic layer. With each exposure to the plasma, the organic monolayer was damaged and consequently the NP's density was gradually reduced. Indeed, when the density of NPs was reduced, T_C decreased monotonically. The plasma process effect on the bare sample was small compared to Fig. 2(a) results. Similar effects of the NP's densities are also presented in the inset of Fig. 2(b), where the results of the 50 nm sputtered Nb film coated with 10 nm NPs linked by the disilane are presented. A clear difference in the critical temperature is seen for the two different densities of adsorption: the high density is approximately 6×10^{10} NP/cm² while the low density is 3 times lower.

For a sample with density of approximately 6×10^{10} NP/cm², the superconducting phase transition was measured at different magnetic fields. The density of the

vortices increases with the magnetic field [15] and the T_C of the sample decreases. At a magnetic field of about 1 T, the density of the vortices matches the density of the NPs. Around this “matching field” the T_C enhancement is reduced, as is evident by comparing Fig. 2(b) (9000 G data) with the inset (0 G data). We relate the shoulder in $R(T)$, measured at 9000 G on the bare Nb film (blue line with squares in the top inset), to the vortex creep mechanism [16]. The disappearance of the shoulder after the attachment of the Au NPs indicates that the NPs provide efficient pinning centers, manifesting their electrical coupling to the Nb film.

The above results suggest that unique coupling occurs between the electrons in the Nb film and in the NPs, mediated by the organic linkers. Such an effect is expected to manifest itself by modification of the electronic density of states (DOS) of the NPs and/or of the Nb film. To study this effect, we performed electron tunneling spectroscopy measurements, using STM, on the various samples described above, at 4.2 K and at 15 K (below and above T_C). Zero-bias anomalies, mostly peaks but occasionally also gaps in the DOS, were observed below T_C for samples in which the NPs caused a change in T_C .

Figure 3 shows two STM dI/dV versus V tunneling spectra acquired at 4.2 K on a 10 nm diameter. In this case the Au NPs (shown to the left of the spectra) were linked to a 50-nm-thick Nb film via disilane molecule. Such tunneling spectra, which are proportional to the local DOS, were numerically derived from I - V curves that were acquired while momentarily disconnecting the STM feedback loop (I - V curves are presented in Fig. 4 of the Supplemental Material [11]). The figure presents a pronounced zero-bias peak observed below T_C only, when

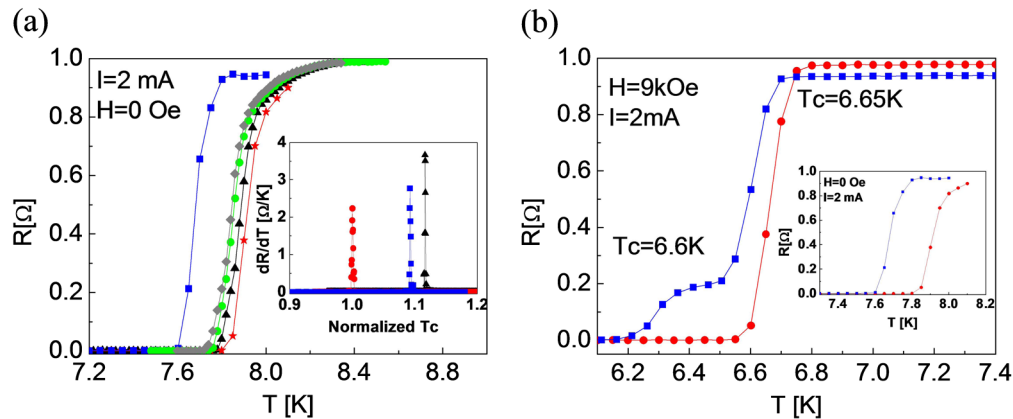


FIG. 2 (color online). (a) $R(T)$ characteristics for 150 nm Nb film: Blue (squares)—bare Nb substrate, red (stars)—after disilane adsorption and 10-nm Au NPs deposition. $R(T)$ curves were then measured for the same sample, after partial removal of the organic layer and the Au NPs by plasma. Black (triangles)—after 10 min plasma cleaning, green (circles)—after 20 min plasma cleaning, and gray (diamonds)—after 60 min plasma cleaning. The data were obtained by applying a current of 2 mA. No effect of the plasma cleaning was seen on the bare Nb film. Inset: The critical temperature of the 50 nm sputtered Nb film coated with 10 nm NPs linked by the disilane at two different densities; the high density is approximately 6×10^{10} NP/cm², while the low density is 3 times lower. (b) $R(T)$ curves before (blue squares) and after (red circles) the Au NP's attachment measured at 9000 and 0 G (inset), close to the matching field, showing smaller T_C enhancement.

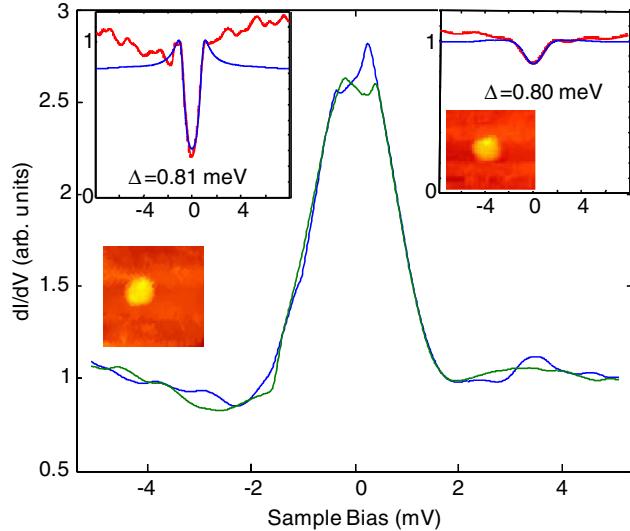


FIG. 3 (color online). Tunneling spectra acquired at 4.2 K on top of a single Au NP of 10 nm diameter (shown to the left) linked to a 50 nm Nb film via disilane molecules, exhibiting the main spectral feature observed—a zero-bias peak. The top right inset presents a spectrum (red top wiggling line) acquired on a gold NP attached to MPS (shown in the inset), exhibiting a proximity-induced gap, while the spectrum presented in the left inset was taken on the MPS covered Nb surface. The blue lines are fits to the Dynes function (see text), with the indicated gaps. The STM images were taken with set values $V = 100$ mV and $I = 0.1$ nA, while the spectra were measured with set bias of 5 mV. The topographic images are 50 nm wide.

measuring on Au NPs in samples that exhibit T_C enhancement. Above T_C , this peak vanished and the spectra became featureless (metalliclike). It is important to note that the appearance of such zero-bias peaks was independent of the STM bias or current set points (before disabling the feedback loop), thus excluding the possibility that they are related to single electron charging effects [17]. The STM setting could affect, however, the peak width and height (see Supplemental Material [11]). The tunneling spectra, measured over the organic layer far from Au NPs (in all samples), showed small gaps such as the one presented in the left inset of Fig. 3. Fitting such a gapped conductance spectra to the Dynes DOS formula [18], $\rho(E) = |\text{Re}(\frac{E-i\Gamma}{[(E-i\Gamma)^2 - \Delta^2]^{1/2}})|$, yielded superconducting gap values Δ in the range 0.81–0.85 meV, somewhat smaller than the largest gaps reported for bare Nb surface, ~ 1.2 meV [19], and relatively large broadening parameters, $\Gamma \sim 0.32$ meV, probably due to the presence of the organic molecules.

We occasionally found very shallow induced proximity gaps on NPs linked to the Nb via the short MPS molecules, along with the conductance peaks observed on most of the other NPs. Such a gap is presented in the right inset of Fig. 3 and could be fitted to $\Delta = 0.8$ meV and $\Gamma = 1.4$ meV. This may relate to our observation that the

MPS molecules can lead to either enhancement or reduction in T_C typical of the conventional PE (see Supplemental Material [11]). It should also be pointed out that the absence of single electron charging effects, in this sample, suggests that the chemically linked NPs are well coupled electronically to the Nb film. In samples where the NPs were physisorbed on the OTS molecules, a different behavior was observed and the tunneling spectra frequently exhibited single electron charging effects [17].

The observed T_C enhancement effect is robust and does not depend (qualitatively) on the sample preparation procedure or the T_C of the bare Nb film (for the same film thickness). However, the magnitude of this effect does depend on the film thickness, the NP size, and the degree of coupling between the NPs and the Nb film.

Several mechanisms were discussed in the literature that may contribute to the observed effect. Among them are enhancement of superconductivity by Anderson localization induced by pair pinning in the vicinity of the NPs [20], or suppressing the surface phonon effect that tend to reduce the T_C of the bare thin Nb films [21]. Another approach is to relate our results to a mechanism suggested by Leggett [22] for high T_C superconductors, [22,23] in which Coulomb interaction between neighboring CuO_2 planes changes the Cooper pairing Hamiltonian and thus increases the interplane coupling. In our case, Coulomb interaction between the Nb film and in the gold NPs may influence the Cooper pairing. The T_C increase may also be attributed to the coupling between the electron states on the Au NPs and electrons in the Nb, which introduces mixing of states without significant charge transfer. Such mixing may give rise to the zero-bias anomalies observed in our tunneling spectra. This approach is related to the Ginsburg prediction [24], which was proposed for geometry similar to ours. The theory explaining this mechanism is outlined in the Supplemental Material [11].

In conclusion, we experimentally measure an enhancement of the critical temperature, which occurs when gold NPs are linked chemically to a superconducting Nb thin film. The observed effect depends on the NPs' size, the length of the organic linkers, and the Nb film thickness. Tunneling spectra acquired on the linked NPs, below T_C , exhibited typically zero-bias peaks and occasionally, for the shorter linkers only, also induced proximity gaps. There are several mechanisms that may explain the observations, among them a pairing mechanism that involves coupling between electrons at the gold NPs and on the Nb film, mediated by the vibrations of the organic linker molecule. However, the aforementioned mechanisms do not explicitly account for the peak in the density of states observed in the tunneling spectra.

Y.P. acknowledges the support of the Peter Brojdie Center. R.N. and B.Y.S. acknowledge support of the

Israel Science Foundation. O.M. thanks DIP 563363 and BSF 2008085 for support. N.K. acknowledges support of ISF 1835/07 and BSF 2008438.

*Corresponding author.

paltiel@cc.huji.ac.il

- [1] P.G.D. Gennes, *Superconductivity of Metals and Alloys* (Westview, New York, 1999), 2nd revised ed.
- [2] A. Frydman and Z. Ovadyahu, *Europhys. Lett.* **33**, 217 (1996).
- [3] A. Y. Kasumov, M. Kociak, S. Guéron, B. Reulet, V.T. Volkov, D. V. Klinov, and H. Bouchiat, *Science* **291**, 280 (2001).
- [4] S. De Franceschi, L. Kouwenhoven, C. Schonenberger, and W. Wernsdorfer, *Nature Nanotech.* **5**, 703 (2010).
- [5] O. Bourgeois, A. Frydman, and R.C. Dynes, *Phys. Rev. Lett.* **88**, 186403 (2002).
- [6] O. Yuli, I. Asulin, O. Millo, D. Orgad, L. Iomin, and G. Koren, *Phys. Rev. Lett.* **101**, 057005 (2008).
- [7] M. Brust, D. Bethell, C.J. Kiely, and D.J. Schiffrin, *Langmuir* **14**, 5425 (1998).
- [8] E. Berg, D. Orgad, and S. A. Kivelson, *Phys. Rev. B* **78**, 094509 (2008).
- [9] T. Kommers and J. Clarke, *Phys. Rev. Lett.* **38**, 1091 (1977).
- [10] M.G. Blamire, E.C.G. Kirk, J.E. Evetts, and T.M. Klapwijk, *Phys. Rev. Lett.* **66**, 220 (1991).
- [11] See Supplemental Material at <http://link.aps.org/supplemental/10.1103/PhysRevLett.108.107004> for more information on the preparation process, STM measurements, and suggested theory.
- [12] S. Yochelis, E. Katzir, Y. Kalcheim, O. Millo, and Y. Paltiel (to be published).
- [13] D. Shvarts, M. Hazani, B.Y. Shapiro, G. Leituss, V. Sidorov, and R. Naaman, *Europhys. Lett.* **72**, 465 (2005).
- [14] E. Katzir, S. Yochelis, and Y. Paltiel, *Appl. Phys. Lett.* **98**, 223306 (2011).
- [15] A. A. Abrikosov, *Sov. Phys. JETP* **5**, 1174 (1957).
- [16] M.W. Coffey and J.R. Clem, *Phys. Rev. Lett.* **67**, 386 (1991).
- [17] A. E. Hanna and M. Tinkham, *Phys. Rev. B* **44**, 5919 (1991).
- [18] R. C. Dynes, V. Narayanamurti, and J. P. Garno, *Phys. Rev. Lett.* **41**, 1509 (1978).
- [19] P.L. Richards and M. Tinkham, *Phys. Rev.* **119**, 575 (1960).
- [20] I. S. Burmistrov, I. V. Gornyi, and A. D. Mirlin, *Phys. Rev. Lett.* **108**, 017002 (2012).
- [21] J. Noffsinger and M.L. Cohen, *Phys. Rev. B* **81**, 214519 (2010).
- [22] A.J. Leggett, *Phys. Rev. Lett.* **83**, 392 (1999).
- [23] A.J. Leggett, *J. Supercond.* **19**, 187 (2006).
- [24] V.L. Ginzburg, *Sov. Phys. Usp.* **19**, 174 (1976).